

Contactless Measurement of Integrity of Silicone Coating on Self-Expandable Esophageal Nitinol Stents

Martin Kopeček^{1,*}, Jiří Záhora¹, Aleš Bezrouk¹

ABSTRACT

Objectives: A stent is a mesh tube inserted into a natural passage in the body to prevent disease induction. Self-expandable esophageal nitinol stents such as SX-ELLA Stent Esophageal HV (HV Stent Plus) can be indicated for palliation of malignant esophageal strictures, for the treatment of benign esophageal strictures that are refractory to standard therapy and for the treatment of esophago-respiratory fistulas. A silicone-stent coating is used for tumor in-growth prevention and esophago-respiratory fistula occlusion. The thickness of the stent and the overall integrity of the silicone coating of all wires indicate the overall mechanical properties of the esophageal stent and the resistance to external adverse events such as corrosion and mechanical and chemical resistance.

Methods: The polymer multicomponent epoxy resin – a mixture of Epon and Durcupan – was used as a method for robust sample stabilization. A cutting system using a thin water beam with a powder (Blue Line) was chosen as the best variant to obtain 6 samples for both-sided measurement (10 measuring sides). The optical microscopic reflective light method was used to examine wire crossing points in the sections. Fifty values were measured on either sample side for the internal, external and mesh thickness of the silicone stent layer. The wire crossing points were selected so that the silicone layer structure could be clearly seen, and the wires approached each other most closely. Only approximately 4 to 8 crossing points in each section could be measured when applying this approach. The resolution of the microscope and calibration (based on the camera used) was 0.677 $\mu\text{m}/\text{pixel}$.

Results: Additional data could be obtained on 8 planes. Two boundary samples were destroyed by the cutting process. Whole coating of the stent was around all mesh wires, especially in areas with higher mechanical stress (wire crossing). The minimum detectable and admissible value determined for all 3 measuring areas (internal, external, mesh) on the wire crossings was 6.77 μm , i.e., 10 pixels, based on the microscope resolution and manufacturer's methodology. The results were characterized by $p < 0.001$ for all 3 parameters. We tested opposite samples in each section to verify the section quality and data consistency. For the 4 areas, the data were significantly different, but the thickness differences were only on the order of units percent, so the measurements were not appreciably affected. We assume that the material cutting loss, making up 1–2 mm, contributed to the differences in the sections.

Conclusion: We examined the overall integrity of the silicone coating of the esophageal stent. The method of HV stent anchoring in a polymeric bath followed by cutting with a waterjet and sample measurement under an optical microscope proved to be very simple and reliable. Sufficient thicknesses of the silicone layer on the wire cross sections were verified. The coated silicone layer thickness appeared to be significantly different along the stent from the proximal part to the distant part, presumably due to the manufacturing technology.

KEYWORDS

nitinol; stent; self-expandable; memory materials; CNC technology; epoxy resin; contactless; optical method; silicone coating

AUTHOR AFFILIATIONS

¹ Department of Medical Biophysics, Charles University, Faculty of Medicine in Hradec Králové, Hradec Králové, Czech Republic

* Corresponding author: Department of Medical Biophysics, Charles University, Faculty of Medicine in Hradec Králové, Šimkova 870, 500 03 Hradec Králové, Czech Republic; e-mail: kopecem@lfhk.cuni.cz

Received: 22 November 2021

Accepted: 23 March 2022

Published online: 29 June 2022

Acta Medica (Hradec Králové) 2022; 65(1): 18–24

<https://doi.org/10.14712/18059694.2022.11>

© 2022 The Authors. This is an open-access article distributed under the terms of the Creative Commons Attribution License (<http://creativecommons.org/licenses/by/4.0>), which permits unrestricted use, distribution, and reproduction in any medium, provided the original author and source are credited.

INTRODUCTION

Self-expandable nitinol stents are made of a metal alloy of nickel and titanium (TiNi 50%) with specific properties, such as shape memory, hyperelasticity, superelasticity, and biocompatibility, that are useful for medical applications, especially for long-term use. The problem is that a tumor can easily penetrate through the stent mesh and the esophageal liquids cause the mesh corrosion. Prevention of tumor in-growth and occlusion of esophagorespiratory fistulas can be achieved by a silicone coating (1). In case of a faulty coating, nitinol wires may contact tissue and cause serious problems with the introduction and use of HV Stent Plus. Over time, the uncovered portion of the nitinol stents could be expanded. The tear of the protective silicone layer could be ruptured and start occlusion in the esophagus-respiratory fistula (2, 3).

Morphological properties and coating thickness were mostly monitored by scanning electron microscopy (SEM) (4, 5). The great advantage of this observation method is that it is very accurate and there is a good contrast of the silicone layer to the background. However, a major disadvantage is a way of cutting the nitinol wire, where the silicone is moved along the wire when the stent is deployed.

To eliminate deformations caused by stent division due to different physical properties of the nitinol stent and the coating, we proposed a method using embedding the stent in resin and subsequent cutting of the sample using a water jet with an abrasive powder. In this paper, we present the results of using this method to measure an HV Stent Plus by an optical microscopy method. Our method tries to verify the integrity of the protective silicone layer of nitinol wires, their crossing, and the space of the mesh windows too (6). The covering of the HV Stent Plus is made of durable silicone and ELLA-CS manufactures all its stent silicone covers in the same way. The mandrel with the stent attached to it rotates around its own axis at a predefined constant speed. The injection needle moves along the surface of the stent at a predefined height in one direction - from the proximal to the distal part. The speed of movement and delay time at the beginning and end of the procedure can be changed, as can the total amount of silicone applied.

No unambiguous conclusions have been reached to date concerning the adequacy of stent skeletons covered with silicone for this stent type. These parameters are under investigation and are important for the verification of production processes.

In our study, we present a new method using the optical microscope to measure thickness and detect failures in silicone coating of nitinol stents. This issue has not yet been addressed by scientific attention in detail (7), and the solution described in this work is unique and original.

MATERIAL AND METHODS

We used commercially available SX-ELLA Stent Esophageal HV - HV Stent Plus (Fig. 1) made from nitinol alloy with silicone coating for the in vitro tests. Stent (Fig. 1) was 85 mm long (L_N), 25 mm in diameter at the stent flares (D_1) and 20 mm at the middle of the stent (D_2).

The method is based on the three general steps. The laboratory compounds and chemical preparation of the sample are described in the first part. A multicomponent epoxy resin was used as a supporting fixative medium. In the second part, the method describes the CNC technology for high-pressure waterjet material division of the stent without destroying the silicone layer (8-10). The last, most important part describes the process of measuring the integrity of the silicone coating by an optical motorized advanced research microscope. The primary outcomes are evaluation of the laboratory protocol and verification of the accuracy of the manufacturing process.

Several methods were proposed to measure the thickness of the silicone coating of the esophageal HV Stent Plus (11), but it was not possible to objectively evaluate the accuracy of the measurements - it was not possible to compare the measured values with other physical quantities. Therefore, the optical measurement method with the Nikon Eclipse 90i and NIS-Elements AR 3.20 - Imaging Software was selected for our precise measurement. The soaking or deposition system for mandrel rotation induces targeted inhomogeneity in the thickness of silicone with different geometries of the proximal and distal portions. A rapid quantitative evaluation of a homogeneous surface

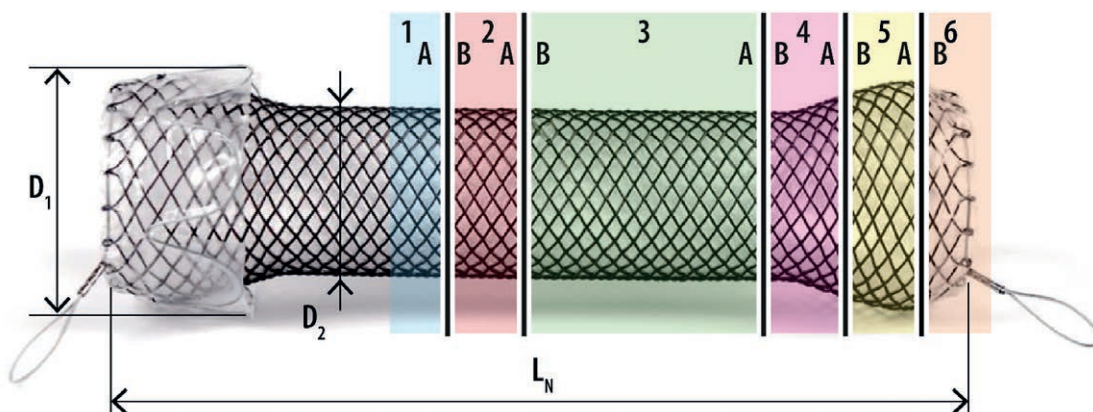


Fig. 1 Slices of areas in HV Stent Plus. The numbers with colored parts are samples, and each sample has two sides. The stent passes from the left-hand proximal part to the right-hand distal part.

coating is the goal of many manufacturers. This connection of cleverly applied methodology with the applied sphere is very desirable.

A. SAMPLE POLYMERIZATION

HV Stent Plus was cut into several sections, as shown in Fig. 1, to measure the thickness of the silicone layer. Thanks to this process, it was possible to measure the thickness at different sites of the HV Stent Plus and at various wire intersections. The initial intention was to cut the HV Stent Plus with special shears, but the wires would roll out and the HV Stent Plus would lose its shape. Cutting the sample preparation with the shears resulted in the HV Stent Plus rolling out, and the integrity of the silicone with the wires was compromised. It was also inappropriate to use deep freezing and subsequent cutting with a laboratory grinder. In these experiments, the silicone layer was torn and could not be kept in direct contact with the wire.

There was only one right option to avoid destroying the material and still have a smooth cut. HV Stent Plus was embedded into a plastic laboratory measuring cylinder and soaked in resin. HV Stent Plus was embedded by using multicomponent epoxy resin – a mixture of Epon and Durcupan ACM (12). (One component is Epon 812 (13), and the other three are durcupan series). The compound was mixed for approximately 40 minutes by an electromagnetic shaker. After embedding (in our case – in the truncated plastic cylinder), the specimen was left for 3 days with a thermostat set at 60 °C, which made the final polymerization of the resin. This method of preparation is unique in the area of stent measurement. Cured epoxy resin without air bubbles acts as a support material.

B. SLICING

An abrasive waterjet cutting method was used for the preparation of the samples. Cutting (10, 14) was performed using CNC technology for high-pressure waterjet material division (Blue Line – Rychly TOM Ltd. Company) with a positioning precision of 0.02 mm, as is partly described in (15). The quality (precision) approached that attained by conventional machining. A beam of high-pressure water with the addition of abrasives is used for controlled grinding of a particular material. Owing to the principle

of this technology, the material is unaffected by any thermal effects, in contrast to other applicable cutting methods (laser, plasma, oxyfuel cutting). The cutting gap thickness when using a hydroabrasive beam is between 0.8 mm and 2.5 mm. The sample cutting procedure involves minimum jet force acting on the material, no microcracks are formed and a high-quality cut, free from burrs, is obtained. This helped create smooth cuts where the nitinol wires (16), silicone and support resin were not mostly destroyed, as shown in Figure 2.

C. CONTACTLESS MEASUREMENT METHOD

Samples were selected that were qualitatively appropriate and usable, and for which it was possible to distinguish individual layers in the cut. Their final selection is shown in Fig. 1. Using an optical microscope, the thickness of the silicone layer was gradually measured at 5x magnification. The final image was measured as shown in Fig. 3. In (17), the authors demonstrate uniform density and integrity of the silicone covering nitinol stent arms and coat the stent wire mesh even at wire crossings. It can be assumed that the wire was cut crosswise during sample preparation; however, for a general view of the stent, we cannot determine from the study whether this silicone is indeed uniformly applied everywhere. We take these facts into account and broaden our knowledge of the properties of the HV Stent Plus coating by using the optical method with a high observed data density.

All the important and evaluable areas were selected at each cut and measured by our optical method. Therefore, we obtained a large amount of data for different distances between wires (wire spacing – mesh) and internal and external thicknesses for silicone around wires, as shown in Fig. 4. The results could be further processed statistically for a large amount of data.

The first step was to determine the minimum silicone layer thickness. We used a Nikon LU Plan Fluor 5x/0.15 objective with a resolution of 0.278 μm . The resolution obtained by combination with the DSFI1 camera was 0.677 $\mu\text{m}/\text{pixel}$ based on the manufacturer's calibration. We set the minimum silicone layer thickness at 10 times the microscope resolution, i.e., 6.77 μm to ensure that we have available an adequately wide range of silicone layer thicknesses evaluable by the conventional method.

Therefore, 6.77 μm is the minimum detectable layer thickness for which we can determine if the silicone coating is present at the point measured. In other words, we can decide whether the wire is fully silicone-coated. The manufacturer does not have the specified minimum thickness of the applied layer, and there is no standard for this. The ideal thickness of silicone is based only on the manufacturer's technological procedures with emphasis on the distribution of mechanical forces inside the HV Stent Plus.

The measurement of the samples was the second step. The silicone layer was sometimes difficult to read, but the number of wires was large enough to enable areas suitable for measurement to be selected. Thanks to cutting possibilities, 4 samples could be made to measure at both sides. Samples 1 and 6 could not be measured due to destruction during cutting. The applicable samples were described



Fig. 2 Layer integrity of the nitinol wire, silicone coating and resin after waterjet cutting.

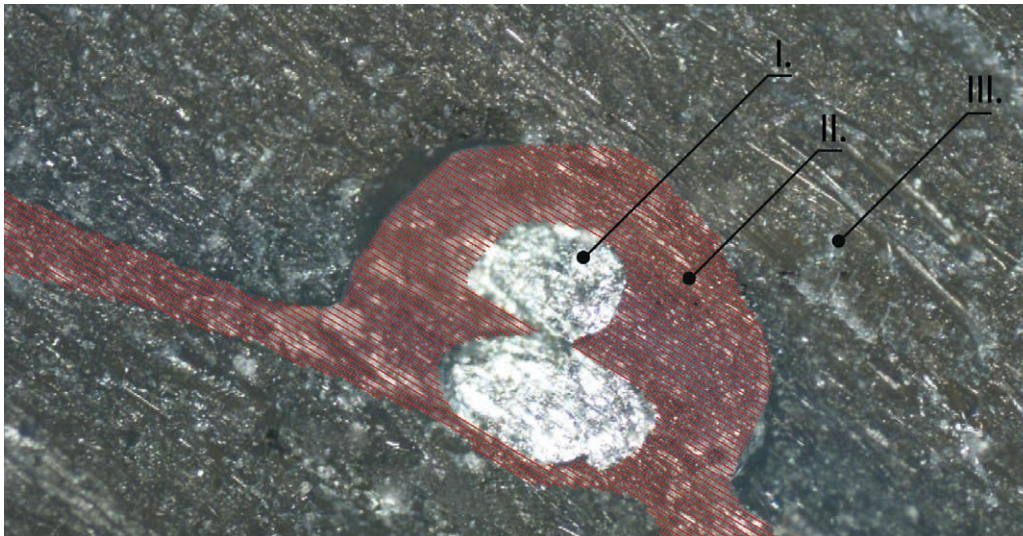


Fig. 3 I is the nitinol wire, II is the silicone layer area around the wire and III is the cured resin. The data define the silicone thickness between the wires.

from both sides and then divided into three groups. Group I includes the values of the 2BA and 3BA sections, samples 4BA and 5B were included in Group II and 5A in Group III. In total, there were 8 plate sides for measurement, and approximately 10 (Fig. 2) crossing wire samples were processed on each side. Four to eight wire crossings from each side were measured 7-10 times (Fig. 4). Number of readings depended on the recognition quality of the silicone/polymer boundary. We decided to measure a total of 50 silicone thickness values at all wire crossings on either side of the section. The details of the crossing of the wire and example of the measurements are shown in Fig. 4.

Redmond, WA, USA) and NCSS 12 (NCSS LLC, Kaysville, UT, USA, ncss.com/software/ncss). We used the D’Agostino omnibus test to test the normality of the data distribution. The data from normally distributed populations were then described using the mean and standard deviation of the sample (\pm SD), while the other data were described using the median and the first and third quartiles of (1st Q, 3rd Q). Since the normality of the distribution of the same shoulder area data was rejected, we opted to use the Wilcoxon signed-rank test because it does not presuppose a normal distribution. A value of $p < 0.05$ was considered to be significant.

D. STATISTICAL ANALYSIS

The external, internal, and mesh coating thicknesses of the corresponding sides of each section were statistically compared using MS Excel 2016 (Microsoft Corp.,

RESULTS AND DISCUSSION

The support resin exhibited negative coloring properties. The epoxy resin did not sufficiently contrast with the

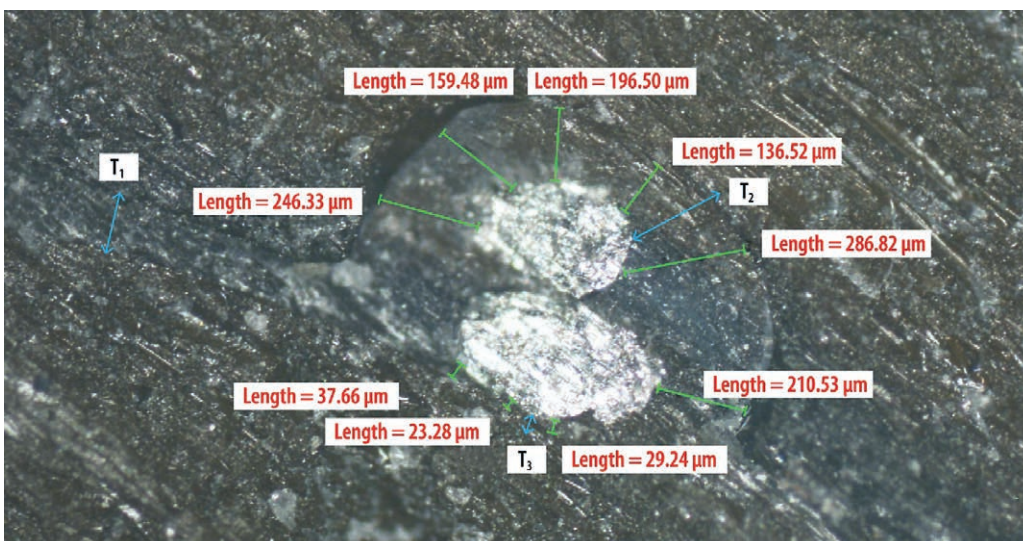


Fig. 4 Three parameters at the cross wire cut. T_1 shows mesh thickness – thickness of the silicone between two wires. T_2 is external thickness – the outside part and T_3 is internal thickness – the inside part of the HV Stent Plus

measured sample, so measurement was difficult at certain points. Additionally, the silicone layer partially absorbed the resin. Sometimes it caused worse readability of the results, sometimes the problem was with poor quality of a section, which affected the image sharpness, and sometimes the section failed to precisely include a wire crossing. Such areas were excluded from measurement. However, it was mostly clear where the boundary between the polymer and the stent was (18). Although HV Stent Plus was precisely laboratory-embedded in the resin, occasionally, despite careful degreasing, it was not possible to directly bond the resin to the silicone layer. This is also evident in Fig. 3, where the silicone layer is not directly in contact with the support. This phenomenon had no effect on the measurement. This is only an effect of insufficient strength of the silicone layer with the resin during the slicing process.

The statistics are borderline. With a larger number of data for only one HV Stent Plus, a greater significance of the differences would be more likely to be achieved. However, the developed method is still acceptable for the intended use in practice. More samples could not be obtained due to the cutting technology used. The stent attachment method in the waterjet cutting machine did not allow for multiple incisions, and no other HV Stent Plus of the same type was available to increase testing. We assume that the manufacturer produces these stents according to standards and certifications of the highest quality. A new stent intended for use in surgery, after passing factory output inspection, was used for the testing. Based on those criteria and regular internal testing by the manufacturer, we believed the stents would have the same properties as the tested product. The deviation is due to the manual stent weaving process because the total surface area of the skeleton material is not constant; hence, the thickness of the silicone layer, the volume of which is always the same for a stent size, may differ by units percent.

The results in Fig. 5 of the silicone coating thickness in the wire intersection show that the minimal measured

value of 11.6 μm was significantly greater than the minimum acceptable thickness given by imaging method parameters – a resolution of 0.677 μm for the microscope and above the minimum value of the verification method of 6.77 μm set by us. The presence of silicone was confirmed by our method for all sections and for all three monitored parameters as internal, external and mesh thickness ($p < 0.001$).

Since we tested the selected sample preparation/cutting method, we made a statistical comparison of the two sides of each section. Statistically significant differences in the silicone coating thicknesses were only identified for the sides of Section 4A vs. 5B ($p < 0.001$) (internal, external and mesh thicknesses) and Section 2A vs. 3B ($p = 0.028$) (mesh thickness). Presumably, the silicone layer thicknesses are different due to the coarse cut with the waterjet-powder system, as a result of which the material is partly damaged, and the layer is not as smooth as the undisturbed side. The cutting method may also have contributed to this. The end part of the stent was too small for perfect clamping, and the shorter distal part could travel due to the vibrations associated with the cutting process. Additionally, note that Sections 5B and 4A were obtained by inclined cuts with respect to the ascent to the flares, whereupon the silicone could be more stretched and hence deformed in certain parts of the section. We also partly ascribe the instability of the sections to the material loss from the action of the waterjet, which was 1 mm (based on the technological process and machine setting). The differences in the measurements of the two sides of a section, however, are on the order of units percent only, which is insignificant to the primary verification of the results.

Our results also show different thicknesses of silicone on the distal flare part of HV Stent Plus. We believe that the dispersion is due to the specific stent manufacturing process. Regrettably, we were unable to confirm this because of the manufacturer's IP protection.

Testing of the silicone coating and the corrosion resistance of the stent is elaborated in the study (19) focuses on

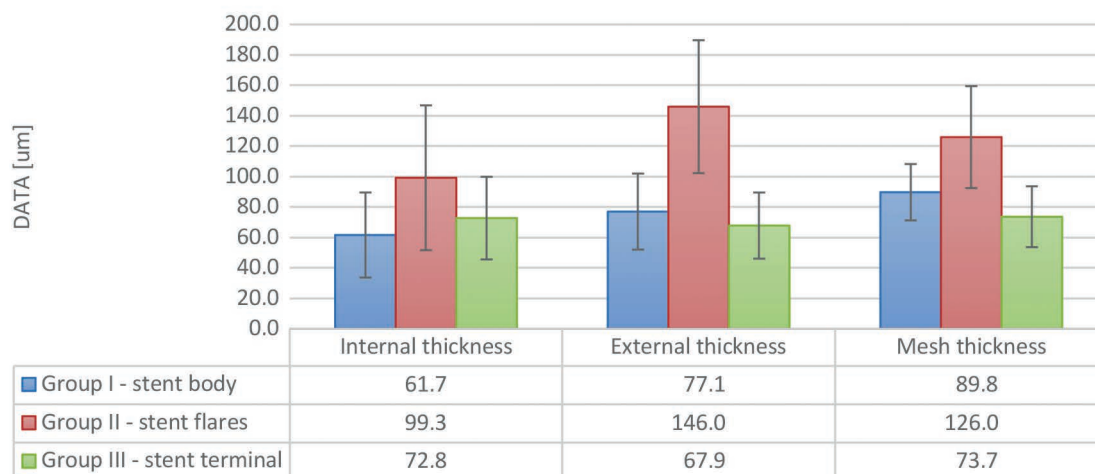


Fig. 5 Comparison of the three monitored thickness parameters: for stent body (Group I), stent flares (Group II) and stent terminal (Group III) with standard deviations. Internal thickness – measurement of the silicone layer on the internal side of the wire. External thickness – silicone thickness on the border of the external side of the wire. Mesh thickness – measurement of the silicone window between the wires.

electrochemical corrosion behavior, which commercial manufacturing companies monitor as undesirable and medically problematic in terms of cracking of uncovered HV Stent Plus. The producer of this stent prepared a set of tests for resistance of silicone against acidic environments to validate the quality of the silicone used. Nine samples of HV Stent Plus were submitted for testing in an acidic environment. The testing solution, which represented an acidic environment in the stomach, was adjusted to $\text{pH} = 3.0 \pm 0.2$. The samples were divided into 3 groups of 3 pcs with immersion times of 4, 8, and 12 weeks. The results of the testing showed no significant changes or damage even after 12 weeks of submersion. On one sample, there were few local silicone covering failures present; however, overall stent integrity was not decreased. Based on the results of the above study, we can conclude that the silicone is very stable, and our resin casting method did not chemically affect it for the reported results.

It would be advisable to try to measure the whole stent from the beginning to the end of the same large segments and to determine the size of the silicone layer over the full length of the esophageal HV Stent Plus in more detail. Another option would be to cut the stent longitudinally and compare these data with already measured results. If advisable, future development of the method will compare the observed data with those from a different stent cutting method and use the results to further improve the HV Stent Plus production output inspection process. No suitable data for this are currently available, and this problem will be addressed in the future. This work is timely due to the occurrence of severe patient injury from uncovered stents, when rupture of nitinol reinforcement followed by cavity perforation of a patient occurred in stents produced by Asian manufacturers (20).

CONCLUSION

We developed a simple and reliable method for the evaluation of stent coating quality. In this method, the stent, embedded in a suitable resin, is cut into parts with a waterjet, and the silicone layer is inspected under an optical microscope. The optical method of measuring the silicone layer of the esophageal HV Stent Plus is further improved and can be applied to further procedures and measurements in the future. The quality and sufficient thickness of the silicone layer in the space of the wire crossing were examined, and it was concluded that the silicone layer was strong enough throughout the body stent, flares and terminal part of the stent. By examining the sides of the section, we were able to demonstrate that the data obtained are reasonably consistent and that the cutting process does not affect the properties to the extent of impacting the final measurement results. Evaluation of the different thicknesses in the area of the flares against the stent body falls under the manufacturer's IP and could not be made in detail. The team thus disproved the possible risk of manufacturing defects in the preparation of esophageal HV Stent Plus and confirmed the correctness of the proposed manufacturing and research procedure. This work is a suitable contribution to optimize the design

and protection of metallic reinforcements with the help of polymers with the consequent possibility of achieving sufficient homogeneity of the coating and thus validating the process. Overall, the silicone layer thicknesses are consistent with the manufacturing technology used by the manufacturer. Therefore, our measurement validated the manufacturing process and final product quality.

ACKNOWLEDGEMENTS

We would like to thank our laboratory staff and Mrs. Zora Komarkova from the Department of Histology and Embryology of our Faculty for her invaluable help.

This work was supported by the programme PROGRES Q40-09 and programme SVV-260397/2021.

FUNDING

None.

CONFLICT OF INTEREST

The esophageal HV Stent Plus was lent by ELLA-CS, s.r.o., Hradec Kralove, Czech Republic. The authors declare that there is no conflict of interest.

REFERENCES

1. Kozarek R, Baron TH, Song H-Y. Self-expandable stents in the gastrointestinal tract. 1st ed. New York, NY: Springer, 2013: 310.
2. Inbar R, Santo E, Subchi AE-A, et al. Insertion of removable self-expanding metal stents as a treatment for postoperative leaks and perforations of the esophagus and stomach. *Isr Med Assoc J* 2011; 13: 230-3.
3. Hirdes MMC, Siersema PD, Houben MHMG, Weusten BL a. M, Vleggaar FP. Stent-in-stent technique for removal of embedded esophageal self-expanding metal stents. *Am J Gastroenterol* 2011; 106: 286-93.
4. Park C-H, Tijging LD, Shon HK, Kim CS. Silicone-coating of nitinol stent wires by electrospinning: catheter deployment test. *Dig J Nanomater Biostruct* 2014; 9: 1-6.
5. Kim HB, Baik KY, Moon MH, Sung CK. Enhanced corrosion resistance of silicone-coated stents by plasma treatment. *Acta Physica Polonica A* 2016; 129: 857-60.
6. Talreja JP, Eloubeidi MA, Sauer BG, et al. Fully covered removable nitinol self-expandable metal stents (SEMS) in malignant strictures of the esophagus: a multicenter analysis. *Surg Endosc* 2012; 26: 1664-9.
7. Hindy P, Hong J, Lam-Tsai Y, Gress F. A Comprehensive review of esophageal stents. *Gastroenterology & Hepatology* 2012; 8: 526-34.
8. Zhang DS, Dong ZW, Chen B, Yang LZ. Development of CNC lower pressure water jet cutter. *Applied Mechanics and Materials* 2010; 37: 349-53.
9. Ramulu M, Arola D. Water jet and abrasive water jet cutting of unidirectional graphite/epoxy composite. *Composites* 1993; 24: 299-308.
10. Li XH, Liao Y, Lei XY, Lu YY, Jiao BQ. Numerically controlled water cutter and its applications in the machining of natural rock materials. *Key Engineering Materials* 2003; 250: 274-80.
11. Classen M, Tytgat GNJ, Lightdale CJ. *Gastroenterological Endoscopy*. 2nd ed. New York: Thieme, 2011: 856.
12. Krenács T, Ivnyi B, Bozky B, et al. Postembedding immunoelectron microscopy with immunogold-silver staining (IGSS) in Epon 812, Durcupan ACM and LR-White resin embedded tissues. *Journal of Histotechnology* 1991; 75-80.
13. Kallivokas SV, Sgouros AP, Theodorou DN. Molecular dynamics simulations of EPON-862/DETDA epoxy networks: structure, topology, elastic constants, and local dynamics. *Soft Matter* 2019; 15: 721-33.

14. Alberdi A, Suarez A, Artaza T, Escobar-Palafox G, Ridgway K. Composite cutting with abrasive water jet. *Procedia Engineering* 2013; 63: 421–9.
15. Unde PD, Gayakwad MD, Patil NG, Pawade RS, Thakur DG, Brahmankar PK. Experimental investigations into abrasive waterjet machining of carbon fiber reinforced plastic. *Journal of Composites* 2015; ID 971596: 1–9.
16. Kong MC, Axinte D, Voice W. Challenges in using waterjet machining of NiTi shape memory alloys: an analysis of controlled-depth milling. *Journal of Materials Processing Technology* 2011; 211: 959–71.
17. Volenec K, Pohl I. The challenges: stent materials from the perspective of the manufacturer. *Gastrointestinal Intervention* 2016; 5: 98–104.
18. Quentin T, Poppe A, Bär K, et al. A novel method for processing resin-embedded specimens with metal implants for immunohistochemical labelling. *Acta Histochemica* 2009; 111: 538–42.
19. Kim Y-S, Kim J-G. Electrochemical corrosion behavior of a non-vascular, bi-stent combination, surgical esophageal nitinol stent in phosphate-buffered saline solution. *Mater Sci Eng C Mater Biol Appl* 2019; 94: 821–30.
20. Lunt CR, Najaran P, Edwards DE, Bell JK, Mullan D, Laasch H-U. The vanishing stent: repeated fracture and dissolution of nitinol gastric stents in a long term cancer survivor. *Gastrointestinal Intervention* 2018; 7: 88–90.